Structure Retention of Silica Gel-Encapsulated Bacteriorhodopsin in Purple Membrane

and in Lipid Nanodiscs

Sukriti Gakhar[‡], Subhash H. Risbud[†], and Marjorie L. Longo*,[‡]

[‡]Department of Chemical Engineering, University of California Davis, Davis, California 95616,

United States

[†]Department of Materials Science and Engineering, University of California Davis, Davis,

California 95616, United States

Keywords: lipid bilayer, lipid nanodisc, hybrid biomaterial, integral membrane protein, sol-gel,

SMA, encapsulation

Word Count: 5,918 words

Figure Count: 8 color figures

Table Count: 0 tables

Abstract

The integral membrane protein, bacteriorhodopsin (BR) was encapsulated in sol-gel derived

porous silica gel monoliths in native purple membrane (BR-PM) and synthetic lipid nanodisc (BR

nanodisc) environments. BR nanodiscs were synthesized by solubilizing purple membrane in

discoidal phospholipid bilayer stabilized by amphipathic Styrene-Maleic Acid (SMA) copolymer.

UV-Visible absorbance spectroscopy and dynamic-light scattering indicated the formation of BR

monomers solubilized in lipid nanodiscs 10.2±0.7 nm in average diameter. Fluorescence and

absorbance spectroscopic techniques were utilized to probe conformational, environmental, and

rotational changes associated with the tryptophan residues and the covalently-bound retinal moiety of BR upon entrapment in the silica matrix. We show that the immobilized BR in both membrane environments retained its bound retinal cofactor and the ability of the cofactor to undergo conformational changes upon light illumination necessary for BR's activity as a proton transporter. For purple membrane fragments, the results indicated that the local pH in the pores around BR after encapsulation was important for its stability at temperatures higher than 50 °C. Under the same buffering conditions, retinal was released from silica-encapsulated BR-PM and BR nanodiscs beginning at 80 °C (without a conformational change) and 50 °C (with a conformational change), respectively, reflecting differences in protein-protein (trimeric vs. monomeric) and protein-lipid interactions.

Introduction

Membrane-associated proteins perform essential biological functions as cellular signal transducers, ion channels, receptors and cellular growth mediators. Because of their important functionalities, this class of proteins which includes kinases and G-protein coupled receptors, are key therapeutic targets. Immobilization of integral membrane proteins (IMPs) on solid substrates can lead to development of high-throughput screening devices for drug discovery among many other applications. The traditional immobilization techniques such as physical adsorption, covalent-binding to solid supports or encapsulation in polymer hydrogels have been explored previously with a few receptor proteins. However, the success achieved using these methods is quite limited and there is a need to develop a platform for routine immobilization of membrane-bound proteins. Sol-gel derived nanoporous silica is optically transparent, mechanically robust, and chemically inert. Since the early 1990's, sol-gel processing has been used to entrap water-

soluble proteins, enzymes and antibodies to develop biosensors or chromatography columns.⁷⁻⁹ One of the key challenges in sol-gel processing for bioencapsulation is the evolution of alcohol upon the hydrolysis of the alkoxide precursors, an issue addressed by Ferrer et al in 2002, when they introduced rotary evaporation after hydrolysis to remove the released alcohol.¹⁰

Since the structural integrity of the membrane host is essential to retain the structure and function of a membrane protein, there have been a few studies to develop a viable biomembrane/sol gel structure. Initial studies done with encapsulation of liposomes made with 1,2- dipalmitoyl-sn-glycero-3-phosphatidylcholine (DPPC) indicated there was rupture of liposomes upon entrapment in the silica gels synthesized using tetraethylorthosilicate (TEOS) precursor.¹¹ In the early 2000s, a few membrane-bound proteins were successfully immobilized using the biofriendly modifications to the sol-gel method. ¹²⁻¹⁴ The entrapped membrane proteins were either present as detergent-solubilized membrane fractions like the Spinach Photosystem I¹³ or as proteoliposomes like Bacteriorhodopsin and F₀F₁ ATP Synthase. ¹⁴ Although the entrapped proteins retained activity, the long-term stability of the encapsulated proteins or the liposomes was not studied.

Recently, there has been an interest in amphipathic molecules like Styrene-Maleic Acid (SMA) copolymer to solubilize membrane proteins in their native membranes overcoming the need of any detergent-solubilization. Addition of SMA molecules to a lipid bilayer structure causes spontaneous formation of lipid nanodiscs with a diameter on the order of 10 nm. These lipid-polymer nanodiscs have been used to solubilize membrane proteins by extracting them from cellular membrane fragments either in presence of synthetic lipids, suggesting that there is some retention of native lipids.

Here we study and compare encapsulated Bacteriorhodopsin (BR), a seven transmembrane alpha helical integral membrane protein, with structural similarity to G-protein coupled receptors,

in TMOS-derived silica gel monoliths hosted in native purple membrane (BR-PM) fragments and in DMPC-SMA nanodiscs. Purple membrane (PM) fragments are derived from the cytoplasmic membrane of archea *Halobacterium Salinarum* and are responsible to drive ATP synthesis in the microorganism by generating a proton gradient across the membrane upon light illumination²⁰⁻²¹. BR, the only protein in the purple membrane, is present in a trimeric state organized in a highly ordered two-dimensional hexagonal lattice structure. A retinal chromophore is bound to the protein via a Schiff base to the lysine 216 residue and photo-isomerization from an all-*trans* to 13-*cis* configuration of the retinal initiates the BR photocycle leading to its proton pumping activity²¹⁻²². PM fragments provide a native lipid environment for BR, however, the average size of such fragments is 200 nm which is quite large compared to the mesopores in sol-gel derived materials.

In our previous work, we successfully encapsulated PM fragments in a sol-gel derived titanium dioxide matrix and showed the retention of covalently-bound retinal to the protein structure²³. We showed that the retinal chromophore could undergo light-induced structural changes upon encapsulation and the formed bionanocomposite could be used for hydrogen production under white light by harnessing the activity of the membrane-associated BR. However, we were unable to characterize the structural changes in the protein by probing the local environment around the tryptophan residues using fluorescence spectroscopic techniques due to the presence of Forster Resonance Energy Transfer between tryptophans and titanium dioxide molecules.²⁴ Since sol-gel derived silica is optically transparent and does not have a spectral overlap with tryptophan emission from BR, encapsulation of PM in silica could provide more information about the effects of entrapment on the tryptophan environment. Further, to understand the effect of size of the membrane on protein stability, we solubilize BR in DMPC-SMA nanodiscs which are of a size more compatible with the pore size of silica. In this work, we encapsulated BR-

PM and BR nanodiscs in silica gel monoliths and used absorbance and fluorescence spectroscopic methods to compare both systems with a focus on the thermal stability of bacteriorhodopsin.

Materials and Methods

Details of the sample preparation and experimental measurements provided in Supplementary Material.

Results and Discussion

Light and Dark- Adapted States. The absorbance spectrum of bacteriorhodopsin (BR) in its dark-adapted state undergoes a red-shift with an increase in the extinction coefficient when exposed to light due to isomerization of its retinal chromophore.²⁵ In its dark-adapted state, the retinal cofactor of BR is present as a 13-cis isomer in a 2:1 ratio with all-trans retinal while the light-adapted state of BR comprises of 98.5% all-trans retinal.²⁵ This isomerization upon light absorption initiates the photocycle of the protein, essential to its function as a proton transporter. Figure 1 shows the steady-state UV-Visible absorbance spectrum of BR-PM in solution and in silica gel. The dark-adapted state of BR-PM in 20 mM tris, 100mM NaCl buffer solution had a maximum absorption at 561 nm which shifted to 568 nm in its light-adapted state (Figure 1(A)). For encapsulation of BR-PM, a biocompatible sol-gel method was used to synthesize silica gel monoliths from TMOS precursor. BR-PM encapsulated in silica gel synthesized with a 1:1 volumetric ratio of silica sol: buffer exhibited a similar pattern where the absorbance maximum shifted from 560 nm to 567 nm between the two states (Figure 1(B)). We also observed an increase in the intensity of maximum absorbance of the light-adapted sample compared to the dark-adapted sample for both the protein in solution and in silica. Based on these results, we can conclude that BR-PM upon encapsulation in silica retained its retinal cofactor along with its ability to undergo conformational changes upon photon absorption.

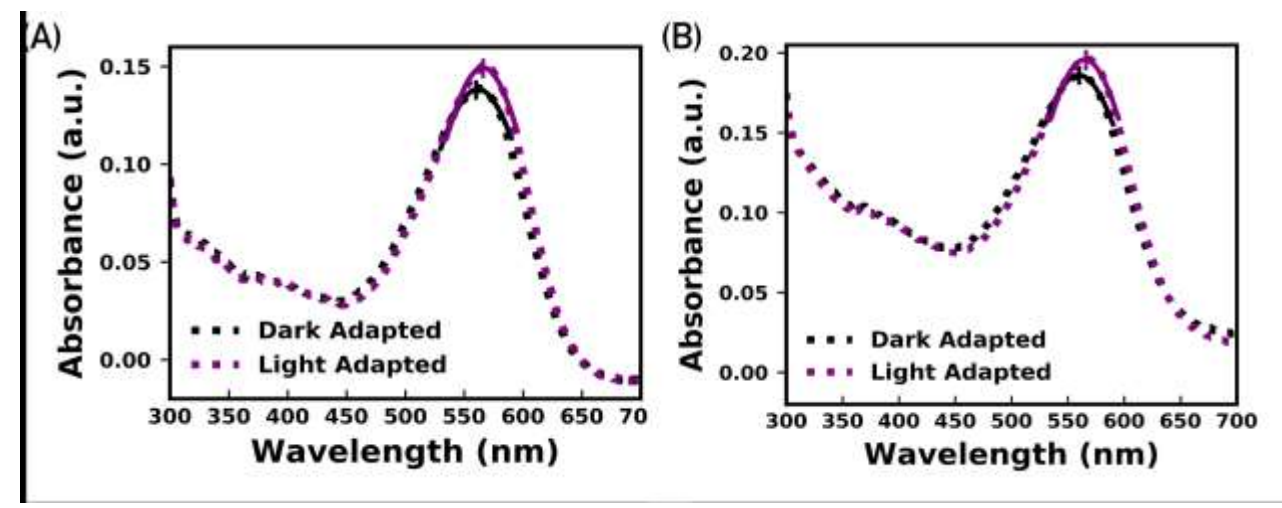


Figure 1. Room temperature steady-state UV-Visible absorbance spectrum of BR-PM in its dark and light adapted states in (A) 20 mM Tris 100 mM NaCl pH 7.4 buffer solution and (B) after encapsulation in silica gel monoliths synthesized with a 1:1 volumetric ratio of silica sol: buffer. The absorbance peaks are marked on the spectra for visualization of the red-shift.

Thermal Stability. Previous studies with encapsulation of water-soluble proteins in sol-gel derived silica have shown that molecular confinement enhances thermal stability of some proteins. 26-27 This is generally attributed to the effect of nanoconfinement on protein unfolding 26. To characterize the effect of silica gel encapsulation on thermal denaturation of BR-PM, intrinsic protein fluorescence was monitored with increasing temperature. Intrinsic fluorescence from the tryptophan residues in a protein is highly sensitive to the changes in the local environment and has been previously used to study temperature induced protein denaturation 28-29. During protein unfolding, as the buried hydrophobic tryptophan residues are exposed to a more polar environment, there is a red-shift in the maximum emission wavelength along with a decrease in the emission

intensity²⁸. BR has 8 tryptophan residues and its intrinsic fluorescence emission intensity and spectrum position is an average of these residues.³⁰ Figure 2(A) shows the normalized fluorescence intensity, measured at 337 nm, for BR-PM in solution and in silica gel with increasing temperature. BR-PM solution emission intensity has a continuous decreasing trend with increasing temperature. The emission intensity at 90°C is approximately 56% of the initial emission intensity measured at 10°C. However, we did not observe a red-shift in the maximum emission wavelength which indicates that the protein structure did not unfold to expose the buried tryptophan residues to the aqueous environment (Figure 2(B), S1(A)). The observed decrease in emission intensity of tryptophan with increasing temperature has been observed previously,³¹ and in the case of a protein, can also be explained with increasing molecular collisions between the excited tryptophans and neighboring quenching groups.²⁸

In contrast to BR-PM in solution, the emission intensity of BR-PM encapsulated in silica gel synthesized with a 1:1 volumetric ratio of silica sol: buffer decreased until 50 °C and then increased until around 75°C. The loss of the retinal leads to this increase in tryptophan emission because in its native state the retinal acts as a quencher for tryptophan fluorescence. Because of their close proximity in the protein structure (<10 nm) there is a very efficient Forster Resonance Energy Transfer (FRET) between the tryptophan residues and the retinal chromophore³². Thus an increase in the separation distance between the two molecules will enhance the tryptophan emission as observed in the thermal denaturation curve for BR-PM encapsulated in the silica (1:1 sol:buffer) sample. Similar to BR-PM in solution, we did not observe a red-shift in the maximum emission wavelength for BR-PM in silica (Figure 2(B), S1(B)). The increase in tryptophan emission however, was coupled with the observation of loss in purple color of the BR-PM in silica gel (Figure 2(A, inset)). Overall, these results indicate that a conformational change does not

accompany the thermally induced disassociation of the retinal chromophore associated with the BR structure in purple membrane. This is represented schematically in Figure 2(C, left to right panel).

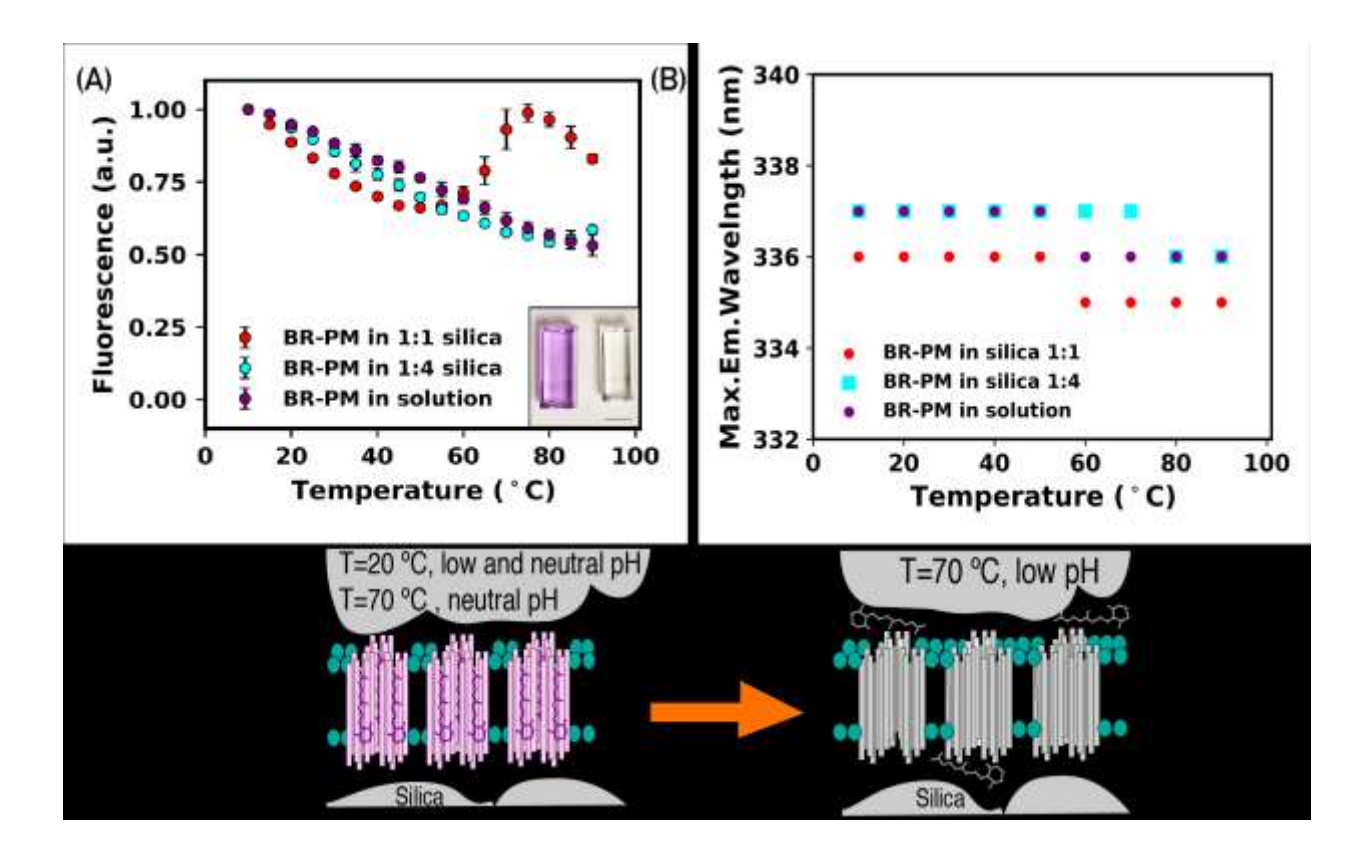


Figure 2. (A) Intrinsic fluorescence emission of BR-PM in buffer solution and in silica gels made with two different sol:buffer volumetric ratios with increasing temperature. The buffer used in these experiments was 20mM Tris, 100mM NaCl, pH7.4. Inset show the sample with BR-PM encapsulated in silica 1:1 (sol:buffer) ratio before and after heating to 90°C showing the loss of purple color associated with the retinal bound to the protein structure (scale bar 1 cm). The fluorescence emission intensity at 337 nm is normalized to the initial value measured at 10 °C for all samples. Error bars represent standard deviation for three samples. (B) The maximum emission wavelength change with temperature for the three samples. (C) Schematic illustration

of the thermally induced retinal disassociation from the BR-PM structure which is not accompanied by a conformational change of the protein. BR is arranged in trimeric form shown along one plane of the larger hexagonal arrangement of the trimers.

Previous work by Neebe et al, suggested that the thermochromic behavior of BR was dependent on pH.33 They demonstrated using temperature-dependent absorbance spectrum of BR that at acidic pH values lower than 4.2, the retinal dissociated from BR at temperatures around 70 °C. To investigate if pH had any effect on our emission results, we encapsulated BR-PM in silica gels synthesized with varying ratios of the silica sol, which intrinsically has a low pH (~3), to tris/NaCl buffer which has a much higher pH (7.4). Silica sol (~ pH 3) was mixed with 20 mM tris 100 mM NaCl buffer (pH 7.4) at volumetric ratios between 1:1 and 1:4 and BR-PM was encapsulated during the gelation process. Fluorescence emission spectra with temperature indicated that the presence of higher amount of pH 7.4 buffer shifted the transition temperature where we begin to see an increase in tryptophan emission to a higher temperature. Figure 2(A) shows that this retinal dissociation transition temperature was increased from approximately 50 °C to 80 °C when comparing BR-PM in silica gels made with 1:1 and 1:4 sol:buffer ratios (Figure S2 for other ratios and different buffer concentrations) and Figure 2(C, left panel) schematically depicts this stability below 80 °C. At 90 °C we did not observe a red-shift in the maximum emission wavelength for BR-PM in silica. (Figure 2(B), S1(C)), indicating, as before, that the retinal dissociated without a change in conformation.

UV-Visible absorbance spectroscopy with temperature was performed to corroborate the results obtained from the tryptophan emission spectra. The appearance of a peak at 380 nm could indicate either hydrolysis of the covalent attachment of retinal to BR³⁴ or deprotonation of the BR-

associated retinal.³⁵ The strong FRET effect discussed above would favor the appearance of such a peak related to hydrolysis and removal of retinal from the BR interior. As shown in Figure 3, temperature-dependent absorbance spectra for BR-PM encapsulated in silica 1:1 (sol:buffer) and silica 1:4 (sol:buffer) reflect the observations made using fluorescence measurements. In the case of the silica 1:1 (sol:buffer) sample (Figure 3(A)), we see there is a remarkable presence of free retinal characterized by a peak at 380 nm at 70°C as compared to BR-PM in silica 1:4 (sol:buffer) (Figure 3(B)). The thermochromic behavior of BR-PM in silica 1:4 (sol:buffer) is more similar to BR-PM in solution at pH 7.4 (Figure 3(C)). The insets in Figure 3 show the two silica gel samples containing BR-PM after heating to 70°C during the absorbance measurements. We see in Figure 3(B) the retention of the purple color associated with properly folded BR in silica 1:4 (sol:buffer) gel while in Figure 3(A) the silica 1:1 (sol:buffer) gel becomes completely transparent. This result suggests that the pH or the buffering capacity at higher temperatures is playing a significant role in influencing the retention of the retinal molecule. In addition, based on the work of Neebe et al, we can tentatively conclude that the pH local to the protein was below 4.2 and above 4.2 for the 1:1 and 1:4 (sol:buffer) ratios, respectively, based upon the presence and lack of free retinal at approximately 70°C.

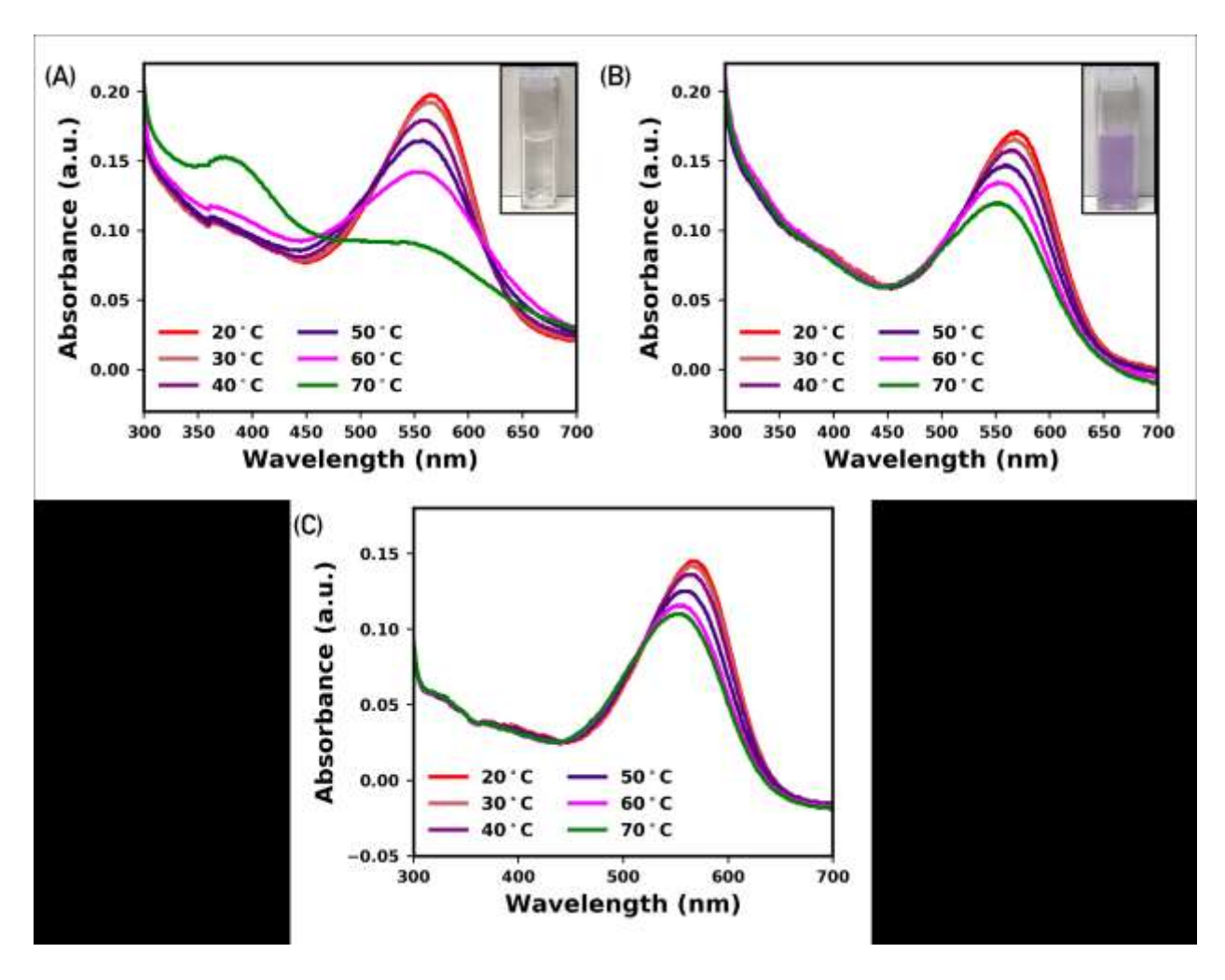


Figure 3. Temperature dependent steady-state UV-Visible absorbance spectrum of BR-PM in silica gel with sol:buffer volumetric ratio (A) 1:1, (B) 1:4 and (C) in buffer solution (20 mM tris, 100 mM NaCl, pH7.4). Absorbance maximum around 565 nm shows the presence of retinal bound to Bacteriorhodopsin and the peak at 380 nm shows the presence of free retinal. Insets show the two silica gel monoliths containing BR-PM after heating the samples to 70°C. BR in silica 1:1 (sol:buffer) doesn't retain the characteristic purple color while the silica 1:4 (sol:buffer) sample still retains its bound-retinal.

The combined results from temperature dependent fluorescence and absorbance spectroscopy show that BR-PM did not show improved resistance to thermal denaturation after

encapsulation in silica gel, unlike some soluble proteins.^{26, 36} In fact, optimization of gelation conditions became necessary to ensure similar thermal stability of the protein in the gel in comparison to the protein in solution. Previous studies with sol-gel immobilization of soluble proteins have shown that the local pH experienced by the protein inside the pores of silica could be lower than the bulk pH by 1 unit even after equilibrating the gel with a buffer for 24-48 hours at the desired pH. ³⁷⁻³⁸ This effect is mainly attributed to the presence of negatively charged silanol groups in the silica matrix at neutral pH and hence, presence of an excess of H⁺ ions in the electric double layer.³⁷ Thus, addition of higher amount of buffer or increasing the buffer concentration proved to enhance the thermal stability of BR-PM, which is sensitive to the pH, after encapsulation. Bacteriorhodopsin Nanodiscs. Styrene Maleic acid (SMA) copolymer has been used to incorporate integral membrane proteins in self-assembled phospholipid bilayer nanodiscs, typically 10-15 nanometer in diameter. ^{16, 18} These SMA nanodiscs are comparable in size with the pores of mesoporous sol-gels and in addition membrane proteins are incorporated into SMA nanodiscs without the denaturing conditions commonly used to reconstitute proteins. PM native lipids are mainly negatively charged phospholipids comprised of phosphatidylglycerophosphate methylated (PGP-Me), phosphatidylglycerol (PG), phosphatidylglycerosulphate (PGS), and archaeal cardiolipin (BPG)³⁹⁻⁴⁰. However, previous work by Knowles et al. established protocols to successfully integrate monomeric BR in nanodiscs stabilized by SMA copolymer using DMPC lipids. 15 Based on these protocols, we solubilized purple membrane in DMPC-SMA nanodiscs, for incorporation into silica sol-gel. Figure 4 shows the Dynamic light scattering data of BR-PM solubilized into DMPC vesicles before and after the addition of SMA polymer. The average particle size for BR-DMPC vesicles is 160.4 ± 44.0 nm (Figure 4(A)) which decreases to $10.2 \pm$ 0.7 nm after SMA addition, followed by centrifugation to remove vesicles and PM fragments

(Figure 4(B)). The insets show the respective samples which undergo a transition from cloudy to clear upon addition of SMA indicating formation of smaller particles. CD spectroscopy of BR-DMPC-SMA nanodiscs by Orwick-Rydmark et al. and Knowles et al. showed that the characteristic biphasic band near the absorbance maxima of trimeric BR in native PM reduces to a monophasic band upon solubilization of PM in DMPC-SMA nanodiscs. This result along with the blue-shift they observed in the absorption maximum of BR from 568 nm in PM to 550 nm upon reconstitution in DMPC-SMA nanodiscs indicated monomerization of BR molecules^{15, 18}. Figure 4(C) shows the absorbance spectrum of the formed BR-DMPC-SMA nanodiscs (BR nanodiscs) which has an absorbance maximum at 548 nm indicating monomerization of BR molecules which exist as trimers in PM with absorbance maximum at 567 nm. In addition, in Figure 5A there exists the presence of a strong intrinsic tryptophan fluorescence emission associated with the BR nanodiscs. These results show the successful incorporation of single BR molecules in the DMPC-SMA nanodiscs. The DLS data and the absorbance spectrum is consistent with the previous literature solubilizing BR in phospholipid bilayer nanodiscs stabilized using SMA copolymers. 15, 18

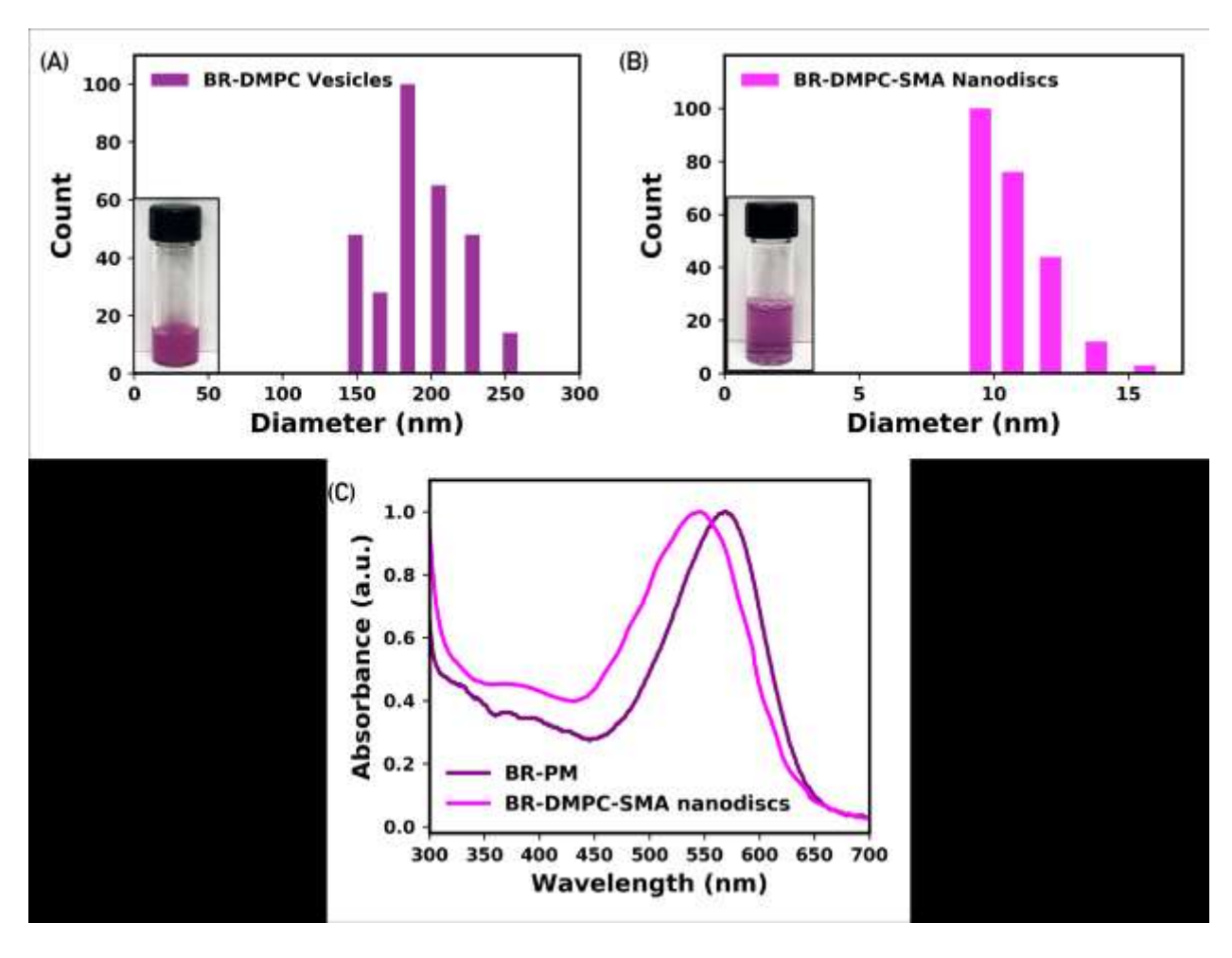


Figure 4. Dynamic light scattering data shows the size distribution of BR-PM solubilized in (A) DMPC vesicles and (B) DMPC-SMA nanodiscs. Insets show the respective samples showing a transition from cloudy to clear solution after addition of SMA block-copolymer. (C) UV-Visible absorbance spectrum of BR-PM and BR-DMPC-SMA Nanodiscs in solution. The blue shift in the absorbance peak indicates monomerization of BR molecules.

The objective after successful formation of BR-DMPC-SMA nanodiscs was to characterize the effect of encapsulation on the protein-nanodisc complex structure in comparison to that of BR-PM. Therefore, we synthesized silica gels encapsulating BR nanodiscs using the sol:buffer ratio of 1:4 based on our results from the stability studies of BR-PM. The steady state UV-Visible

absorbance spectrum of BR nanodiscs both in solution and in silica gel had an absorbance maximum at 545 nm in the dark-adapted state of the protein which is a lower wavelength than the dark-adapted state of BR-PM as expected for monomeric vs. trimeric BR, respectively. Upon light illumination, the absorbance maximum shifted to 550 nm for both samples indicating retention of the chromophore and its ability to undergo photoisomerization (Figure S3). This observation was similar to our results with encapsulated BR-PM.

The effects of immobilization on protein structure were analyzed using intrinsic fluorescence emission of the tryptophan residues in BR nanodiscs. Maximum emission wavelength (λ_m) of tryptophan residues is highly sensitive to its micro-environment. A decrease in polarity of the environment around the residues causes a blue shift in the maximum wavelength Figure 5(A) shows the emission spectra from BR nanodiscs before and after encapsulation in silica gel monoliths. The observed λ_m was 326 nm and 337 for BR nanodiscs and BR-PM, respectively, both in solution and in silica gel. This result suggests that the hydrophobicity around the tryptophan residues did not change after encapsulation. There was a blue-shift in the maximum emission wavelength that was observed in BR nanodiscs compared to BR-PM. However, the emission spectrum of BR monomers, formed by solubilizing PM using surfactants like SDS, was shown to be red-shifted due to an increase in exposure to the aqueous environment. Therefore, the membrane environment of DMPC lipids, rather than the native negatively-charged PM lipids, might have had the dominant environmental effect in enhancing the hydrophobicity around some of the tryptophan residues.

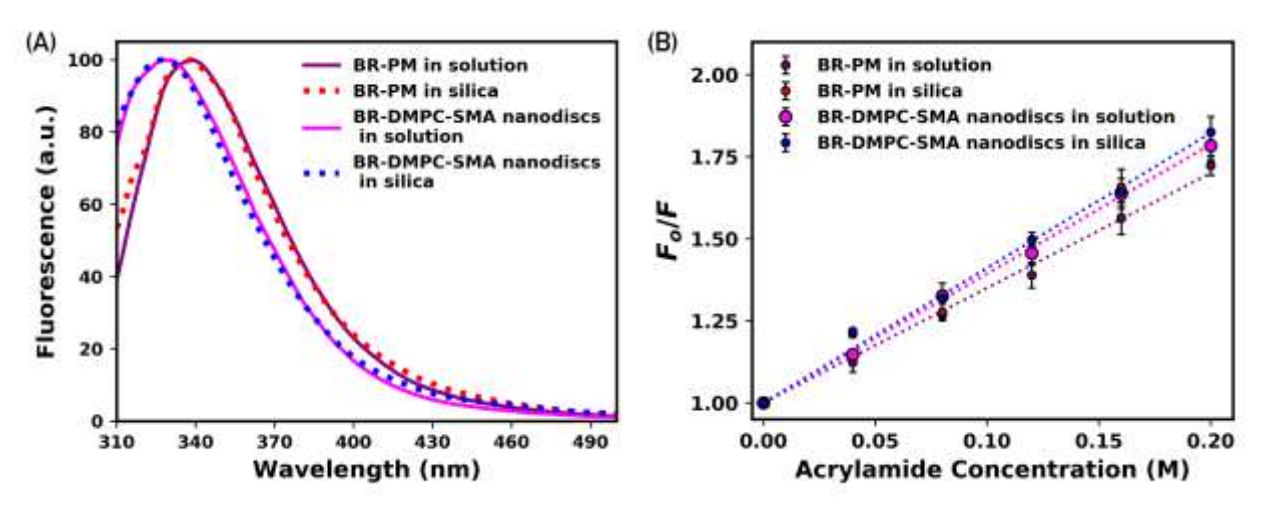


Figure 5. (A) Intrinsic fluorescence emission spectra of BR-PM and BR-DMPC-SMA nanodiscs in solution and after encapsulation in silica gel. (B) Stern-Volmer plots for acrylamide quenching of BR tryptophan residues in different membrane environments. In both A and B silica samples were made with sol:buffer volumetric ratios of 1:4.

Fluorescence quenching of tryptophan residues by acrylamide is used to determine their overall accessibility to the solvent. Quenching experiments were performed on BR nanodiscs in comparison to BR-PM to understand if the tryptophan residues became more or less exposed to water after entrapment in silica gel. The information from the quenching studies could provide information on the effects of confinement on the structural integrity of the protein-nanodisc complex. Figure 5(B) shows the Stern-Volmer plots from acrylamide quenching of BR fluorescence in the two different membrane environments before and after encapsulation. The Stern-Volmer constant, K_s , from the data was calculated to be 3.93 ± 0.26 and $4.10\pm0.21~M^{-1}$ for BR nanodiscs in solution and in silica, respectively. There was no statistically significant difference observed between the quenching constants, suggesting that the exposure of tryptophan residues to the solvent remained the same. Based on the Stern-Volmer constants combined with the λ_m data, we conclude that the BR nanodisc complex retains the lipid-protein interactions upon

encapsulation in silica gel at room temperature. Stern-Volmer constants regressed from the quenching data of PM before and after encapsulation in silica gel were calculated to be 3.5 ± 0.24 and $3.94\pm0.27~M^{-1}$, respectively indicating a similar result with no significant change in the solvent exposure of tryptophan residues. Since there is no significant difference in the K_s values of BR nanodiscs and BR-PM, the more exposed tryptophan residues are in a similar environment in BR nanodiscs and BR-PM. Therefore, the blue shift observed in λ_m could be caused by a more hydrophobic environment for the more buried tryptophans in the protein structure rather than those closer to the protein surface.

Thermal Stability of BR Nanodiscs. The effect of silica gel encapsulation on the thermal stability of BR nanodiscs was investigated using fluorescence spectroscopy in a similar manner to the BR-PM stability study. As shown in Figure 6(A), for both BR nanodiscs in solution and BR nanodiscs in silica gel 1:4 (sol:buffer), we see a non-monotonic trend for intrinsic emission intensity with temperature. The emission intensity decreases until around 50 °C which is then followed by an increase in emission intensity until 75 °C. However, the emission intensity increases approximately 200% more for BR nanodiscs in solution compared to BR nanodiscs in silica. As mentioned earlier, the increase in distance associated with the loss of retinal from the protein structure diminishes the energy transfer from the tryptophans to the retinal, leading to an increase in the observed emission. Therefore, an emission increase reflects both extent of release of retinal from BR and the subsequent distance between the two molecules. Along with a change in the maximum intensity, we observed a large red-shift of approximately 5.5 nm in the maximum emission wavelength comparing 10°C and 75°C indicating a more polar environment at 75°C for tryptophan residues for both solution and silica samples (Figure 6(B) and Figure S4). Overall, these results indicate that a conformational change does accompany the thermally-induced disassociation of the retinal chromophore associated with the BR structure in nanodiscs. This is shown schematically in Figure 6(C, left to right panel).

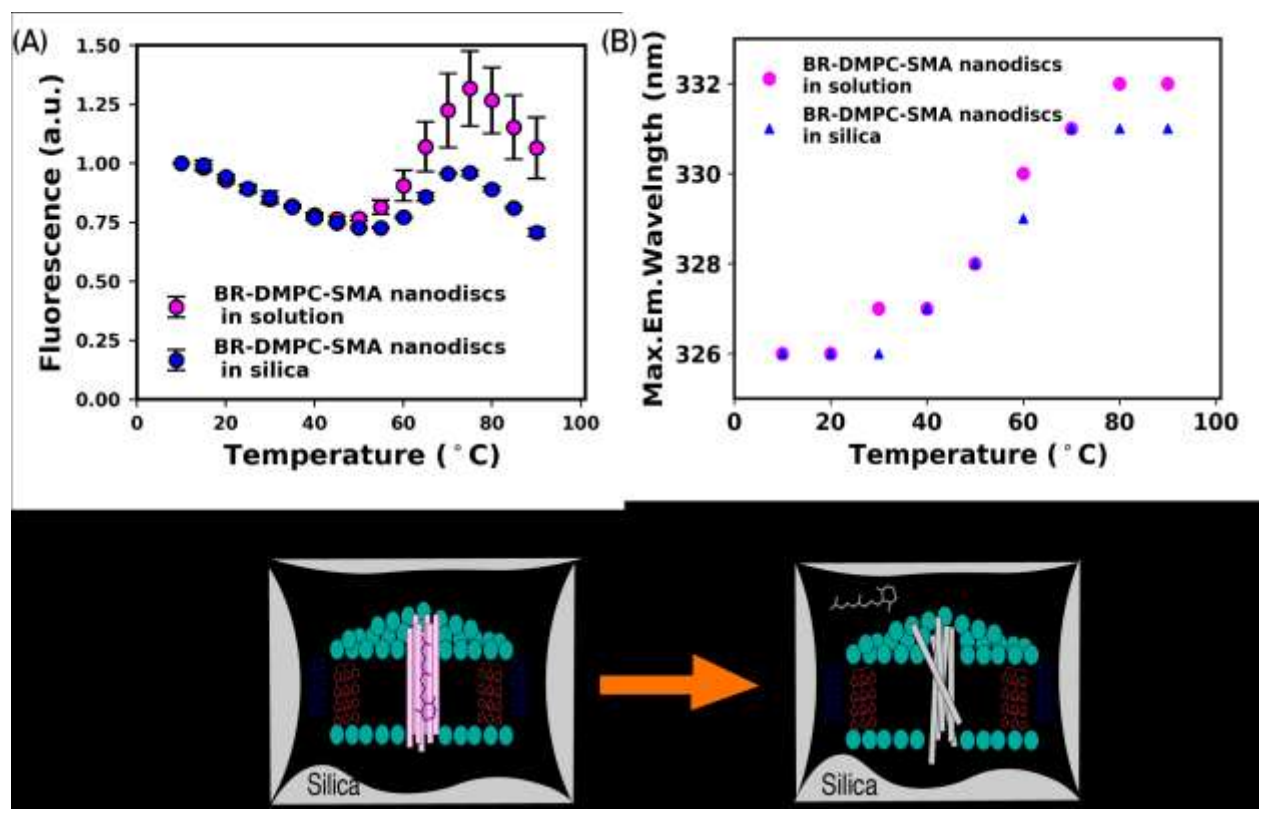


Figure 6. (A) Intrinsic fluorescence emission of BR-DMPC-SMA nanodiscs in solution and in silica gel with increase in temperature. The fluorescence emission intensity at 326 nm is normalized to the initial value measured at 10 °C for all samples. Error bars represent standard deviation for three sample measurements. (B) The maximum emission wavelength change with temperature for the two samples. (C) Schematic illustration of retinal disassociation from the BR in nanodiscs during thermally-induced protein unfolding.

We measured the temperature-dependent UV-Visible absorbance spectra of BR nanodiscs in solution and encapsulated in silica gel in order to gauge whether there is similar release of retinal. Raw absorbance data of BR nanodiscs in solution had an increase in absorbance at

wavelengths between 300-350 nm with increasing temperature (Fig S5(A)). Styrene, associated with the SMA copolymer, has a temperature dependent absorption in this region of the spectrum and therefore this is the most likely source of this spectral feature.⁴³ Indeed, DMPC-SMA nanodisc hosts, in the absence of BR, displayed increased absorbance with temperature (Figure S6(A)) which we later subtracted out (Figure S6(B)) since it interferes with the increase in the free retinal absorption. We ruled out the possibility that the increase in absorbance could be due to light scattering caused by formation of larger vesicles/aggregates. DLS measurements shown in Figure S7, do not show an increase in the average particle size with temperature. Indeed, Jamshed et al. found, by differential scanning calorimetry, high structural integrity of DMPC-SMA nanodiscs even at temperatures as high as 90 °C.⁴⁴ Interestingly, raw absorbance data of BR nanodiscs in silica gel displayed strong absorbance in the styrene region of the spectrum as a result of the presence of SMA copolymer, but did not have an increase in absorbance with increasing temperature (Fig S5(B)).

The data on the temperature-dependent UV-Visible absorbance spectra of BR nanodiscs in solution and encapsulate in silica gel is presented in the form of difference spectra in Figure 7, which eliminates the confounding spectral overlap of the SMA absorption. We see for both BR nanodiscs in solution (Figure 7(A)) and BR nanodiscs in silica gel (Figure 7(B)), there is a decrease in the peak at 550 nm as the temperature increases indicating the loss of the bound retinal moiety accompanying thermal denaturation of the protein. There is also a simultaneous increase in the concentration of the free retinal characterized by the peak at 380 nm for both samples. The extent of these changes, due to retinal loss, are on a similar scale for BR nanodiscs in solution and in silica. Therefore, we postulate that confinement in the silica pores limits the achievable separation

between BR and free retinal explaining the lower, FRET related, fluorescence emission that we observed earlier in Figure 6.

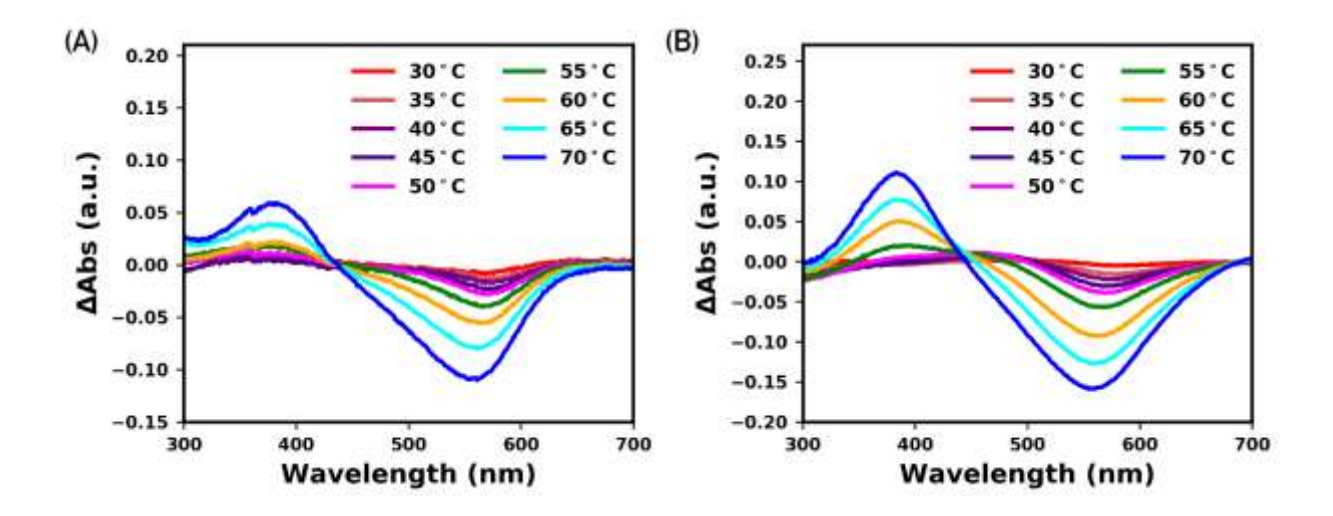


Figure 7. Difference absorbance spectra of BR nanodiscs at temperatures between 30 °C and 70°C in (A) solution (B) silica gel monolith. The absorbance spectrum of each sample at 20°C was used as a reference to calculate the difference spectra after correcting for the temperature-dependent increase in the SMA absorbance in the case of (A).

Another key observation here is that, in silica gel formed under the same conditions, BR in nanodiscs loses the retinal at 50 °C (Figure 6) in contrast to BR-PM (Figure 2) which loses the retinal at a much higher temperature of 80 °C. It has been shown that in wild-type PM BR has a trimeric arrangement and strong lipid-protein packing with high stability against thermal and chemical stresses⁴⁵. Indeed, we found that thermally induced retinal loss was not accompanied by conformational changes of BR-PM, but was accompanied by conformational in the case of BR associated with nanodiscs. Therefore, our results reflect the loss of strong native protein-protein interactions (monomer in nanodiscs vs. trimeric in PM) and diminished lipid-protein interactions as shown for other detergent-solubilized monomeric forms of Bacteriorhodopsin⁴⁶.

Fluorescence Anisotropy of BR Nanodiscs. Steady-state fluorescence anisotropy of tryptophan residues is used to estimate their rotational freedom along with the rotational motion of the protein.⁴⁷ Here, we use anisotropy measurements of tryptophans present in BR to compare their rotational diffusion in different membrane environments before and after encapsulation in silica. As shown in Figure 8, the anisotropy of tryptophan residues in BR-PM and BR nanodiscs was 0.118±0.004 and 0.114±0.005. This is not a statistically significant difference and we can conclude that the overall mobility of tryptophans in BR did not change in the two membrane structures. After entrapment in the pores of silica gel 1:4 (sol:buffer), the anisotropy increased to 0.131±0.008 and 0.171±0.006 for BR-PM and BR nanodiscs, respectively. This increase suggests that the rotational movement in the pores is restricted for both BR-PM and BR nanodiscs, although the effect is more pronounced for BR nanodiscs. During gelation, a pore in the 10 nm size range typically forms around the biomolecule that is in the solution⁴⁸. The size of BR nanodiscs (12 nm) compares well with the pore size, which could explain the enhanced effect of molecular confinement on the observed anisotropy. Similar results have been shown for water-soluble proteins upon encapsulation in mesoporous materials⁴⁹. In comparison, BR-PM are essentially large inclusions in the silica gel in which the BR molecules likely retain much of their native lipid and protein environment diminishing the influence of confinement.

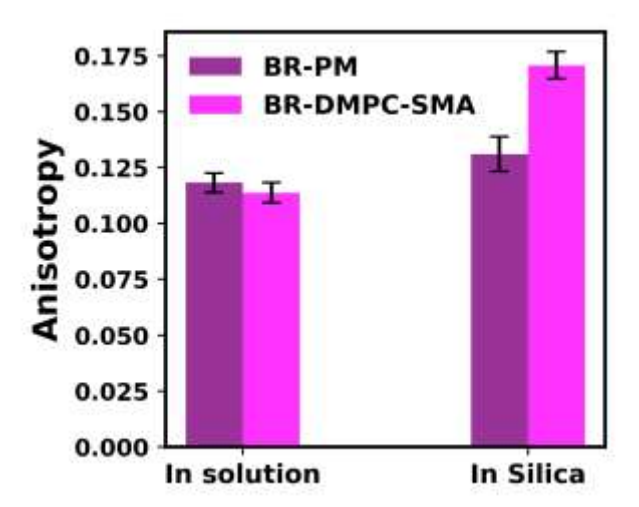


Figure 8. Fluorescence anisotropy values of BR tryptophan residues in PM and DMPC-SMA nanodiscs before and after encapsulation in silica gel 1:4 (sol:buffer). The error bars represent standard deviation of 10 measurements from each sample.

Conclusions

Fluorescence and absorbance spectroscopic techniques applied here indicate that, under optimized encapsulation conditions, BR in both membrane environments was rotationally restricted but did not have significant structural changes upon entrapment in the pores of the silica gel at temperatures below 50 °C. Our findings provide the first experimental evidence that an integral membrane protein hosted by a lipid bilayer nanodisc retains its structure when encapsulated in a silica gel, and more broadly, sets the stage for future work on immobilization of membrane proteins using lipid nanodiscs as hosts in sol-gel derived porous materials.

AUTHOR INFORMATION

Corresponding Author

*E-mail: mllongo@ucdavis.edu

ACKNOWLEDGEMENTS

MLL, SHR, and SG acknowledge support from the National Science Foundation under award number DMR - 1806366. We are grateful to the laboratories of Prof. Karen McDonald and Prof. Michael Toney for the use of their UV-Visible spectrophotometers.

SUPPLEMENTARY MATERIAL

Materials and methods and supplementary figures.

REFERENCES:

- 1. Guidotti, G., In *Physiology of Membrane Disorders*, Andreoli, T. E.; Hoffman, J. F.; Fanestil, D. D., Eds. Springer US: Boston, MA, 1978; pp 49-60.
- 2. MÜLler, D. J.; Wu, N. A. N.; Palczewski, K., *Pharmacol. Rev.* **2008,** *60* (1), 43-78.
- 3. Hoeller, D.; Volarevic, S.; Dikic, I., Curr. Opin. Cell Biol. 2005, 17 (2), 107-111.
- 4. Besanger, T. R.; Brennan, J. D., J. Sol-Gel Sci. Technol. 2006, 40 (2-3), 209.
- 5. Rogers, K. R.; Valdes, J. J.; Eldefrawi, M. E., *Anal. Biochem.* **1989**, *182* (2), 353-359.
- 6. Kröger, D.; Hucho, F.; Vogel, H., *Anal. Chem.* **1999,** *71* (15), 3157-3165.
- 7. Monton, M. R. N.; Forsberg, E. M.; Brennan, J. D., *Chem. Mater.* **2012**, *24* (5), 796-811.
- 8. Kato, M.; Sakai-Kato, K.; Matsumoto, N.; Toyo'oka, T., *Anal. Chem.* **2002,** *74* (8), 1915-1921.
- 9. Zhang, T.; Tian, B.; Kong, J.; Yang, P.; Liu, B., Anal. Chim. Acta **2003**, 489 (2), 199-206.
- 10. Ferrer, M. L.; del Monte, F.; Levy, D., Chem. Mater. 2002, 14 (9), 3619-3621.
- 11. Besanger, T.; Zhang, Y.; Brennan, J. D., J. Phys. Chem. B **2002**, 106 (41), 10535-10542.
- 12. Besanger, T. R.; Easwaramoorthy, B.; Brennan, J. D., *Anal. Chem.* **2004**, *76* (21), 6470-6475.
- 13. O'Neill, H.; Greenbaum, E., *Chem. Mater.* **2005**, *17* (10), 2654-2661.
- 14. Luo, T.-J. M.; Soong, R.; Lan, E.; Dunn, B.; Montemagno, C., *Nat. Mater.* **2005,** *4* (3), 220.
- 15. Knowles, T. J.; Finka, R.; Smith, C.; Lin, Y.-P.; Dafforn, T.; Overduin, M., *J. Am. Chem. Soc.* **2009**, *131* (22), 7484-7485.
- 16. Lee, S. C.; Knowles, T. J.; Postis, V. L. G.; Jamshad, M.; Parslow, R. A.; Lin, Y.-p.; Goldman, A.; Sridhar, P.; Overduin, M.; Muench, S. P.; Dafforn, T. R., *Nat. Protoc.* **2016**, *11* (7), 1149-1162.
- 17. Dörr, J. M.; Scheidelaar, S.; Koorengevel, M. C.; Dominguez, J. J.; Schäfer, M.; van Walree, C. A.; Killian, J. A., *Eur. Biophys. J.* **2016**, *45* (1), 3-21.
- 18. Orwick-Rydmark, M.; Lovett, J. E.; Graziadei, A.; Lindholm, L.; Hicks, M. R.; Watts, A., *Nano Lett.* **2012**, *12* (9), 4687-4692.
- 19. Long, A. R.; O'Brien, C. C.; Malhotra, K.; Schwall, C. T.; Albert, A. D.; Watts, A.; Alder, N. N., *BMC Biotechnol.* **2013**, *13*, 41-41.
- 20. Shiu, P.-J.; Ju, Y.-H.; Chen, H.-M.; Lee, C.-K., *Protein Expression Purif.* **2013**, *89* (2), 219-224.
- 21. Henderson, R., *Annu. Rev. Biophys. Bioeng.* **1977,** *6* (1), 87-109.
- 22. Haupts, U.; Tittor, J.; Oesterhelt, D., *Annu. Rev. Biophys. Biomol. Struct.* **1999,** *28* (1), 367-399.

- 23. Johnson, K. E.; Gakhar, S.; Deng, Y.; Fong, K.; Risbud, S. H.; Longo, M. L., *ACS Appl. Mater. Interfaces* **2017**, *9* (41), 35664-35672.
- 24. Johnson, K. E.; Gakhar, S.; Risbud, S. H.; Longo, M. L., *Langmuir* **2018**, *34* (25), 7488-7496.
- 25. Scherrer, P.; Mathew, M. K.; Sperling, W.; Stoeckenius, W., *Biochemistry* **1989**, *28* (2), 829-834.
- 26. Eggers, D. K.; Valentine, J. S., *Protein Sci.* **2001**, *10* (2), 250-261.
- 27. Chen, Q.; Kenausis, G. L.; Heller, A., J. Am. Chem. Soc. 1998, 120 (19), 4582-4585.
- 28. Permyakov, E. A.; Burstein, E. A., *Biophys. Chem.* **1984,** *19* (3), 265-271.
- 29. Luong, Trung Q.; Verma, Pramod K.; Mitra, Rajib K.; Havenith, M., *Biophys. J.* **2011**, *101* (4), 925-933.
- 30. Plotkin, B. J.; Sherman, W. V., Biochemistry 1984, 23 (22), 5353-5360.
- 31. Gally, J. A.; Edelman, G. M., *Biochim. Biophys. Acta* **1962**, *60* (3), 499-509.
- 32. Alexiev, U.; Farrens, D. L., *Biochim. Biophys. Acta* **2014**, *1837* (5), 694-709.
- 33. Neebe, M.; Rhinow, D.; Schromczyk, N.; Hampp, N. A., *J. Phys. Chem. B* **2008**, *112* (23), 6946-6951.
- 34. Cladera, J.; Galisteo, M. L.; SabÉS, M.; Mateo, P. L.; PadrÓS, E., *Eur. J. Biochem.* **1992,** *207* (2), 581-585.
- 35. Druckmann, S.; Ottolenghi, M.; Pande, A.; Pande, J.; Callender, R. H., *Biochemistry* **1982**, *21* (20), 4953-4959.
- 36. Lan, E. H.; Dave, B. C.; Fukuto, J. M.; Dunn, B.; Zink, J. I.; Valentine, J. S., *J. Mater. Chem.* **1999,** *9* (1), 45-53.
- 37. Bhatia, R. B.; Brinker, C. J.; Gupta, A. K.; Singh, A. K., *Chem. Mater.* **2000**, *12* (8), 2434-2441.
- 38. Dunn, B.; Zink, J. I., *Chem. Mater.* **1997,** *9* (11), 2280-2291.
- 39. Grigorieff, N.; Beckmann, E.; Zemlin, F., J. Mol. Biol. 1995, 254 (3), 404-415.
- 40. Renner, C.; Kessler, B.; Oesterhelt, D., J. Lipid Res. **2005**, 46 (8), 1755-1764.
- 41. Vivian, J. T.; Callis, P. R., *Biophys. J.* **2001**, *80* (5), 2093-2109.
- 42. Ng, K. C.; Chu, L.-K., J. Phys. Chem. B **2013**, 117 (20), 6241-6249.
- 43. Müller-Markgraf, W.; Troe, J., J. Phys. Chem. **1988**, 92 (17), 4914-4922.
- 44. Jamshad, M.; Grimard, V.; Idini, I.; Knowles, T. J.; Dowle, M. R.; Schofield, N.; Sridhar, P.;
- Lin, Y.; Finka, R.; Wheatley, M.; Thomas, O. R. T.; Palmer, R. E.; Overduin, M.; Govaerts, C.; Ruysschaert, J.-M.; Edler, K. J.; Dafforn, T. R., *Nano Res.* **2015**, *8* (3), 774-789.
- 45. Imhof, M.; Pudewills, J.; Rhinow, D.; Chizhik, I.; Hampp, N., *J. Phys. Chem. B* **2012,** *116* (32), 9727-9731.
- 46. Brouillette, C. G.; McMichens, R. B.; Stern, L. J.; Khorana, H. G., *Proteins* **1989**, *5* (1), 38-46.
- 47. Lakowicz, J. R.; Maliwal, B.; Cherek, H.; Balter, A., *Biochemistry* **1983**, *22* (8), 1741-1752.
- 48. Macmillan, A. M.; Panek, D.; McGuinness, C. D.; Pickup, J. C.; Graham, D.; Smith, W. E.; Birch, D. J. S.; Karolin, J., *J. Sol-Gel Sci. Technol.* **2009**, *49* (3), 380-384.
- 49. Nabavi Zadeh, P. S.; Åkerman, B., J. Phys. Chem. B **2017**, 121 (12), 2575-2583.

Graphical Abstract

